

# **Robot Calibration with Planar Constraints**

**Hanqi Zhuang\*, Shui H. Motaghedi\*\* and Zvi S. Roth\***

**\*Department of Electrical Engineering  
Florida Atlantic University  
Boca Raton, FL 33431**

**\*\*Jet Propulsion Laboratory  
California Institute of Technology  
4800 Oak Grove Drive  
Pasadena, California 91109**

## **Abstract**

This paper investigates issues related to robot calibration with planar constraints and, in particular observability conditions for the parameters of the kinematic model of the robot. Both single- and multiple-plane constraints for robot calibration are considered. It is shown that a single-plane constraint is normally insufficient for calibrating a robot. It is also shown that by using a three-plane constraint, the constrained system is equivalent to an unconstrained point-measurement system under certain conditions. The significance of this result is that one can use the three-plane constraint setup to successfully calibrate a robot. Simulation results are provided that verify the theory presented.

# 1 Introduction

Robot calibration is a process of robot accuracy enhancement built to a high level of mechanical repeatability. It encompasses compensation for absolute accuracy deficiencies using internal compensation software. Basic steps in a robot calibration task include kinematic modeling, pose measurement, identification and compensation [ 1 ]. This paper focuses on the measurement phase of robot calibration.

Various pose measurement methods for robot calibration have been developed by researchers and practitioners. Researchers have also been looking for ways to self-calibrate robots without explicit measuring of robot poses. Self-calibration may be done using two alternative strategies. One is to install additional redundant joint-level sensors to the robotic system to facilitate measurement data collection [ 2-3 ]. An alternative strategy is to impose some sort of motion constraints on the end-effector of the robot. Bennett and Hollerbach [ 4 ] proposed a closed-loop calibration method in which the robot endpoint is kept fixed. Mooring was first to propose to the use of a planar constraint to calibrate a laser scanner [5]. Zhuang et al [ 6 ] used planes to constrain the target motion for the calibration of a multiple-beam laser tracking system. Ikits and Hollerbach [ 7 ] extended their Implicit Loop Method to the plane constraint method. Recently, a method to calibrate a Stewart platform using data collected solely by robot internal sensors has been proposed by Khalil and his coworkers [8].

A planar constraint method for robot calibration may be classified into single-plane and multiple-plane constraints. In this paper, parameter observability issues associated with both methods are explored. The results can be applied to robots as well as other programmable machines. It is shown in this paper that whenever a single plane constrains the robot motion, the calibration result is biased because the measurement data is projected to a particular direction. Furthermore, a single-plane constraint does not necessarily guarantee the observability of unknown kinematic parameters of the robot.

A multiple-plane constraint is a remedy to this limitation. It is shown in the paper that under certain conditions, data collected by a three-plane constraint setup is equivalent to that by a point measurement device. The significance of this observation is that one may replace a 3D-position measurement system by a plane placed at a number of different orientations. The calibration strategy of using a multiple-plane constraint is demonstrated on a PUMA 560 robot model.

## 2 Problem Formulation

With a single planar constraint, the calibration problem is reduced to an optimization problem of minimizing a cost function  $C$  of the type

$$C = \sum_{i=1}^m (\mathbf{n} \cdot \mathbf{r}_i(\boldsymbol{\varrho}, \boldsymbol{\theta}) + d)^2 \quad (1)$$

where  $\mathbf{r}_i$  is the vector of the coordinates of the  $i$ th point on the plane,  $m$  is the number of points,  $\mathbf{n}$  is the plane normal,  $d$  is the distance from the origin to the plane,  $\boldsymbol{\varrho}$  is a vector consisting of all the unknown parameters of the calibrated system and  $\boldsymbol{\theta}$  is the vector containing the measurements. Unlike the case of using an external measuring device to obtain pose data,  $\mathbf{r}_i$  in this case is not explicitly measured but is rather computed using any suitable forward kinematic convention of the robot characterized by the set of kinematic parameters  $\boldsymbol{\varrho}$ . If the target motion is constrained to multiple planes, the above cost function is extended to

$$C = \sum_{s=1}^{m_p} \sum_{i=1}^{m_s} (\mathbf{n}_s \cdot \mathbf{r}_{s,i}(\boldsymbol{\varrho}, \boldsymbol{\theta}) + d_s)^2 \quad (2)$$

where  $\mathbf{r}_{s,i}$  represents the coordinates of the  $i$ th point on plane  $s$  in a reference frame,  $\mathbf{n}_s$  is the  $s$ th plane normal,  $d_s$  is the distance from the origin to the  $s$ th plane,  $m_p$  is the number of planes, and  $m_s$  is the number of points taken from the  $s$ th plane. The problem is to estimate

$\rho$  so that the above function is minimized. In the case that the plane is placed in unknown locations, the plane parameters must also be estimated along with the robot parameters.

### **3 A single-plane constraint**

#### **3.1 The system setup**

A schematic setup of calibrating a general machine system using a single-plane constraint is shown in Figure 1.

In order for the method to work, it is assumed that the machine is capable of moving its tool-tip on the plane, verifying proper contact between the tool-tip and the plane, and collecting its internal joint position sensor reading at each joint configuration. The number of points measured should exceed the total number of parameters to be calibrated in the entire system. The physical nature of measurement varies from one machine to another. In a laser tracking system, a retroreflecting target is moved along planar constraints, as the gimbal rotation angles and the interferometric relative distance reading between the laser tracker and retroreflector are recorded. In a robotic manipulator system, the end-effector sensory system may take the form of a simple limit switch activated upon contact with the surface, or a proximity sensor (such as a laser “pen”, which indicates the distance between the tool and the surface). The recorded data is that of the robot joint positions. The constraint plane defines a coordinate frame that is different from the machine base coordinate frame. Although either one of the coordinate frames can be chosen as the reference frame, different sets of observability conditions for the system parameters can be derived.

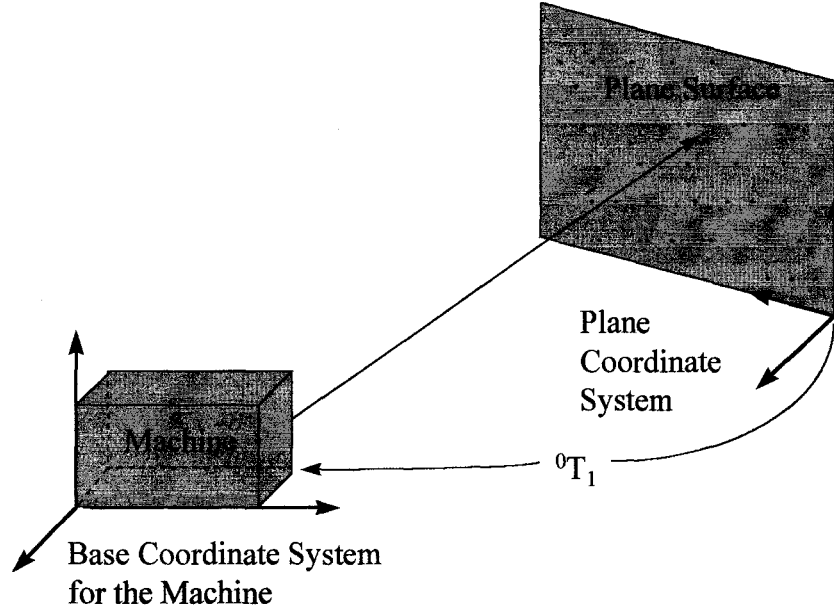


Figure 1 The system setup of robot calibration with a single plane constraint

### 3.2 Observability issues with known plane parameters

Let us first assume that the constraint plane is placed in a known position and orientation with respect to the reference coordinate frame. In other words, it is assumed that the plane parameters are known *a priori* in the reference coordinate frame. To study the observability of the calibrated system, it is necessary to derive an error model of the system.

For  $m$  points measured on the plane, the measurement equation becomes

$$\mathbf{n}^T \mathbf{r}(\rho_a, \theta_i) + d = 0 \quad (3)$$

where  $i$  is the point index between 1 and  $m$ . The augmented machine parameter vector is  $\rho_a = [\rho^T, \alpha^T, \mathbf{p}^T]^T$  where  $\alpha$  and  $\mathbf{p}$  represent the orientation and position parameter vectors of the machine base system in the plane coordinate system (shown in Figure 1), and  $\rho$  is the kinematic parameter vector of the machine.

Linearization of (3) about a nominal kinematic parameter vector  $\rho_a = \rho_a^0$  yields:

$$-n^T J(\rho_a, \theta_i) d\rho_a = n^T r(\rho_a, \theta_i) + d \quad (4)$$

where  $J$  is the Identification Jacobian [ 1, 8 ] of the corresponding unconstrained system<sup>1</sup>. The Jacobian of the constrained system can then be obtained by stacking the Jacobians  $-n^T J(\rho_a^0, \theta_i)$ ,  $i = 1, 2, \dots, m$ , from top to bottom, which is

$$-NJ_a d\rho_a = NR + D \quad (5)$$

$$\text{where } N = \begin{bmatrix} n^T & 0 & \dots & 0 \\ 0 & n^T & \dots & 0 \\ \vdots & 0 & \ddots & \vdots \\ 0 & 0 & \dots & n^T \end{bmatrix}_{m \times 3m}, \quad J_a = \begin{bmatrix} J(\rho_a^0, \theta_1) \\ J(\rho_a^0, \theta_2) \\ \vdots \\ J(\rho_a^0, \theta_m) \end{bmatrix}_{3m \times q}, \quad R = \begin{bmatrix} r(\rho_a^0, \theta_1) \\ r(\rho_a^0, \theta_2) \\ \vdots \\ r(\rho_a^0, \theta_m) \end{bmatrix}_{3m \times 1},$$

$$D = \begin{bmatrix} d \\ d \\ \vdots \\ d \end{bmatrix}_{m \times 1}.$$

It is assumed that the number of measurements  $m$  is always no less than the number of unknown parameters; otherwise, the Identification Jacobian matrix  $NJ_a$  is singular. Equation (5) is a first-order differential error model that relates the parameter error vector to the measurement vector  $NR + D$ . To facilitate the discussion of the observability of the system, let us modify (4) slightly. Let  $J_a = [\mathbf{j}_x^T \mathbf{j}_y^T \mathbf{j}_z^T]^T$ ,  $\mathbf{n} = [n_x \ n_y \ n_z]^T$  and  $\mathbf{r} = [r_x \ r_y \ r_z]^T$ , where  $\mathbf{j}_x$ ,  $\mathbf{j}_y$ ,  $\mathbf{j}_z$  are  $1 \times q$  vectors. Then (4) becomes,

---

<sup>1</sup> Unconstrained system here means that the robot end-effector is not confined to move on a plane and the full pose data of the robot is obtained using an external measuring device.

$$-(n_x \dot{j}_x + n_y \dot{j}_y + n_z \dot{j}_z) d\rho_a = n_x r_x + n_y r_y + n_z r_z + d \quad (6)$$

The reference coordinate system can be assigned in an arbitrary way without loss of generality. Assume for example that the plane lies on the  $yz$  plane of the coordinate system. Therefore the plane normal vector  $\mathbf{n}$  is a unit vector  $[1 \ 0 \ 0]^T$ . Equation (6) is then reduced to

$$-\dot{j}_x d\rho_a \cong r_x + d \quad (7)$$

Either (6) or (7) provides a scalar measurement equation. To be able to compute  $d\rho_a$ , at least  $q$  measurements must be taken. Let  $\mathbf{G} = [\dot{j}_{x,1}^T, \dot{j}_{x,2}^T, \dots, \dot{j}_{x,q}^T]^T$ . It is the Identification Jacobian of the constrained system. Obviously, for each point,  $\mathbf{G}$  only picks up the rows corresponding to the  $x$  element of the Jacobian of the unconstrained system.

The observability of the augmented tracker error parameters is determined in terms of the structure of  $\mathbf{G}$ .  $\mathbf{G}$ , which is a submatrix of the Identification Jacobian of the unconstrained system, is required to be nonsingular. This implies that as a necessary condition for the constrained system to be observable, the unconstrained system should be observable. Moreover, even if the error parameters of the unconstrained system are observable, those of the constrained system may not. This is because even if  $\mathbf{J}_a$  is nonsingular,  $\mathbf{G}$ , which is a submatrix of  $\mathbf{J}_a$ , may still be singular. Let us assume without loss of generality that a fixed coordinate transformation is introduced such that (7) is valid. It is obvious that if  $r_x$  is not a function of some of the kinematic parameters of the robot, the Identification Jacobian will be singular. In other words, these parameters will be unobservable. The following example illustrates this point.

**Example:** Consider a 3 DOF SCARA arm having a RRP joint configuration. Let us further assume that the only kinematic parameters to be calibrated are the joint offsets. Let us assume that the plane is placed such that its surface normal is pointing in the  $x$  direction. Clearly,  $r_x$  is not a function of the offset of the prismatic joint, therefore the prismatic joint offset is not observable.

In conclusion, a single plane constraint is often insufficient for calibrating a robotic manipulator.

### 3.3 Observability issues with unknown plane parameters

There are situations in which the reference frame cannot be defined within the constraint plane. In this case the plane parameters  $\mathbf{n}$  and  $d$  can no longer be assumed to be known. Since  $\{\mathbf{n}, d\}$  constitutes only independent parameters, we may fix  $d$  at its nominal value and assume that the plane normal is not normalized. The unknown parameters of the plane are represented by  $\mathbf{n}$ . Recall that the plane equation is

$$\mathbf{n}^T \cdot \mathbf{r}(\rho^0, \theta) + d = 0 \quad (8)$$

The error model of (8) is then,

$$-\mathbf{r}(\rho^0, \theta)^T d\mathbf{n} - \mathbf{n}^T \mathbf{J}(\rho^0, \theta) d\rho \cong \mathbf{n}^T \mathbf{r}(\rho^0, \theta) + d \quad (9)$$

If  $m$  points are measured on the plane, the Identification Jacobian of the constrained system can be written as

$$[\mathbf{R} \quad \mathbf{NJ}]_{m \times (3+q)} \quad (10)$$

$$\text{where } \mathbf{R} = \begin{bmatrix} \mathbf{r}(\rho^0, \theta_1)^T \\ \mathbf{r}(\rho^0, \theta_2)^T \\ \vdots \\ \mathbf{r}(\rho^0, \theta_m)^T \end{bmatrix}_{m \times 3}, \quad \mathbf{N} = \begin{bmatrix} \mathbf{n}^T & 0 & \dots & 0 \\ 0 & \mathbf{n}^T & \dots & 0 \\ \vdots & 0 & \ddots & \vdots \\ 0 & 0 & \dots & \mathbf{n}^T \end{bmatrix}_{m \times 3m}, \quad \mathbf{J} = \begin{bmatrix} \mathbf{J}(\rho_a^0, \theta_1) \\ \mathbf{J}(\rho_a^0, \theta_2) \\ \vdots \\ \mathbf{J}(\rho_a^0, \theta_m) \end{bmatrix}_{3m \times q}.$$

By examining the structure of the Identification Jacobian given in (10), one observes that in addition to the necessary condition that the unconstrained system must be observable, another condition must be met; that is, measurement points must not all lie on a plane passing through the origin of the coordinate frame (refer to Figure 1). Since the measured points are on a plane, this condition is equivalent to that the measured points on

the plane must not all lie on a line. If the condition is violated, matrix  $\mathbf{R}$  becomes singular, resulting in a singular Identification Jacobian.

## **4 A Multiple-plane Constraint**

The insufficiency of having two planar constraints (for calibration of a robotic manipulator) can be established along the same arguments used to illustrate the inadequacy in general of a single plane constraint. Therefore a “multiple-plane constraint” in this paper will always imply that the number of planes is no less than three.

### **4.1 The System Setup**

A schematic of the robot calibration with multiple-plane constraints is given in the following figure. It is assumed that the planes can be placed at any place in the space. Similar to the single-plane constraint, the machine measures a certain number of points on each plane respectively. From Figure 2, it is noticed that each plane has its own coordinate frame while the machine has its base coordinate frame. In the calibration process, either one of the planar coordinate frame or the machine base coordinate frame will be chosen as the reference frame for the entire system.

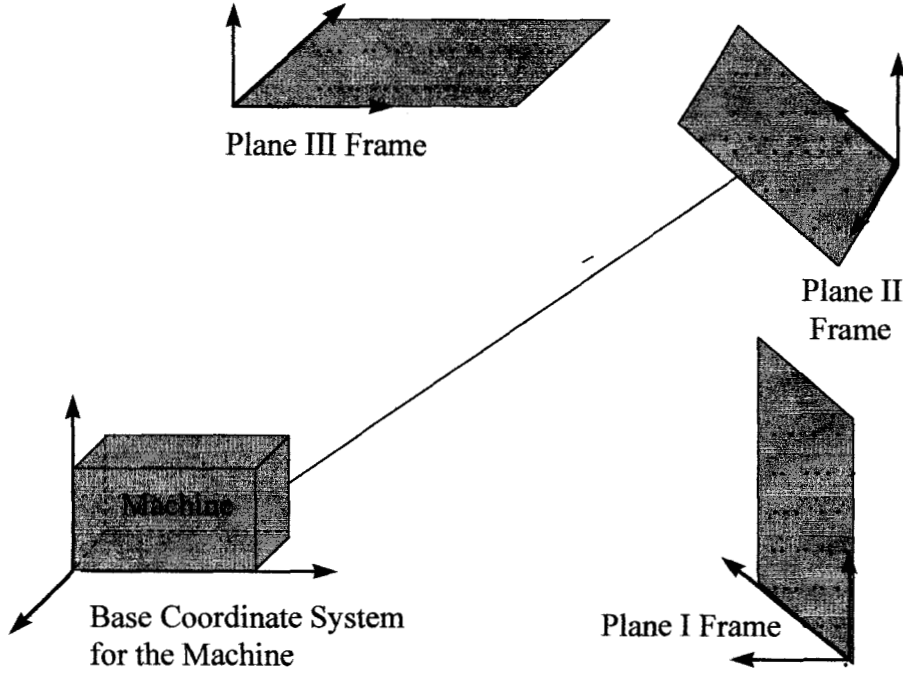


Figure 2 The system set of robot calibration with multiple plane constraint

#### 4.2 Observability issues with known plane parameters

In this section, it is assumed that the plane parameters are known *a priori*. There are three planes in the system and  $m$  points measured on each plane. In order to estimate the unknown parameters, the number of measurements in this case must be no less than one third of the number of unknown parameters of the robot. The observability condition of the constrained system is revealed in the following theorem.

**Theorem 1.** Assume that all measurements are constrained to lie on three mutually non-parallel planes. The full set of error parameters can be made observable if the following Jacobian matrix is nonsingular:

$$\begin{bmatrix} \mathbf{J}_{1x} \\ \mathbf{J}_{2y} \\ \mathbf{J}_{3z} \\ \vdots \\ \mathbf{J}_{(3m-2)x} \\ \mathbf{J}_{(3m-1)y} \\ \mathbf{J}_{3mz} \end{bmatrix}$$

where  $\mathbf{J}_{i,j}$  is drawn from the Identification Jacobian of the corresponding unconstrained point-measurement system.

The proof of the above theorem can be found in the Appendix. The significance of this theorem is that as long as the three planes are all mutually non-parallel, the constrained system offers the same amount of information as an unconstrained position measurement system, as long as the plane parameters are known in a reference plane.

#### 4.3 Observability issues with unknown plane parameters

As a straightforward extension to three unknown planes of the single plane constraint case, a necessary condition for the unknown parameter vector to be observable is that measured points taken from each individual plane must not all lie on a line on that plane. We thus have the following necessary conditions:

1. All three planes are mutually non-parallel,
2. The Identification Jacobian of the unconstrained system is nonsingular, and
3. Measured points from each individual plane do not lie on a line on that plane.

## 5 Calibration of a PUMA Robot

The simulation results shown in this paper will focus only on the multiple-plane constraint case since it was observed in Section 3.2 that a single plane constraint often

does not provide sufficient constraints for error parameter identification. In the simulation, Puma 560 robot is used as a test bed. Readers are referred to [10] for more a detailed description.

## 5.1 Kinematic modeling

Similar to [7], Hayati's modified D-H kinematic model was adopted in the simulation. Let one of the three planes be roughly perpendicular to the first robot axis. The base frame is numbered as -1. The remaining coordinate frames {0} to {6} are placed on the six links of the Puma 560 robot. The definitions of frames {0} through {6} follow the standard DH representation except for frame {2} of the shoulder axis. Figure 3 shows the entire set of coordinate frames. Figure 4 gives a detailed description of frame {-1} through {2}. Frame {2} uses a modified DH representation (Hayati's modification) since joint 2 is nearly parallel to joint 3. After establishing the above coordinate systems, the transformation matrix relating frame {6} to frame {-1} is represented as product of basic homogenous transformation matrices:

$${}^{-1}T_6 = T_{z,d_0} T_{x,\alpha_0} T_{z,\theta_1} T_{x,a_1} T_{x,\alpha_1} T_{z,\theta_2} T_{x,a_2} T_{x,\alpha_2} T_{x,\beta_2} T_{z,d_3} T_{z,\theta_3} T_{x,a_3} T_{x,\alpha_3} T_{z,d_4} T_{z,\theta_4} T_{x,a_4} T_{x,\alpha_4} T_{z,d_5} T_{z,\theta_5} T_{x,a_5} T_{x,\alpha_5} T_{z,d_6} T_{z,\theta_6} T_{x,a_6} T_{x,\alpha_6} \quad (11)$$

where  ${}^{-1}T_6 = \begin{bmatrix} n & o & a & \eta \\ 0 & 0 & 0 & 1 \end{bmatrix}_{4 \times 4}$ . The measured (or computed) end-effector position vector is

$$r = \eta \quad (12)$$

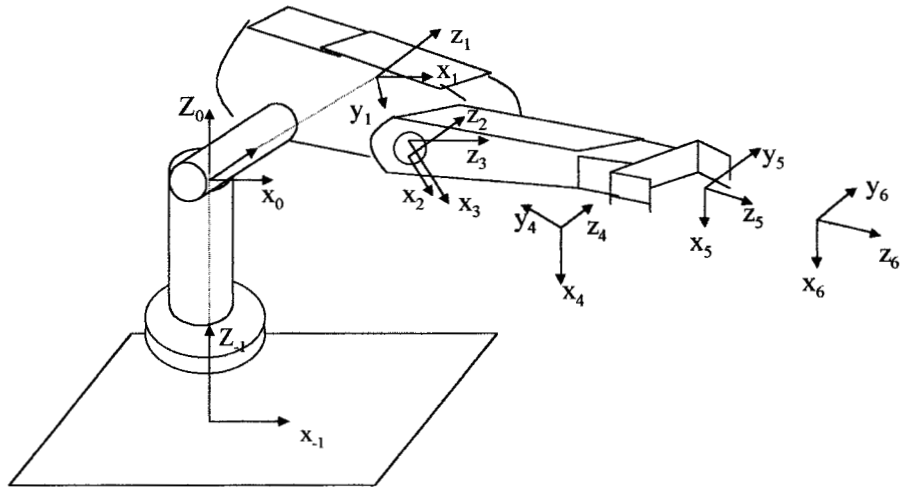


Figure 3 Coordinate systems of a PUMA560 robot

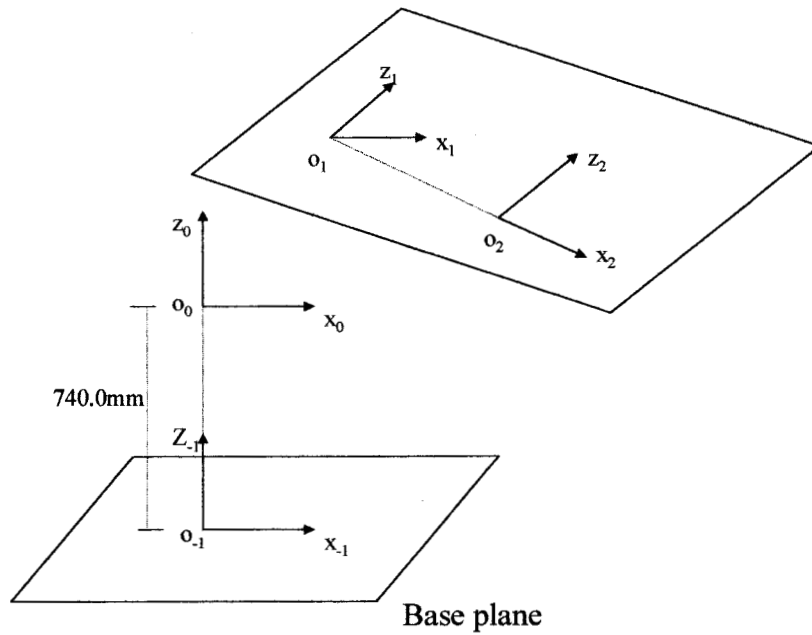


Figure 4 Coordinate systems of the Planes

## 5.2 Simulation Design

Section 5.1 defines only one of the three constraint planes.

Table 1 outlines four setups of the remaining two planes used for calibration and the 4<sup>th</sup> plane for verification. In the first setup, the second plane was obtained by rotating the first plane about the  $x$  axis  $10^\circ$  followed by a 0.3m displacement in the  $z$  direction. The third plane is obtained by rotating the first plane  $-10^\circ$  about the  $x$  axis and  $5^\circ$  about the  $y$  axes and a displacement 0.5m along the  $z$  axis. This setup is illustrated in Figure 5. A 4<sup>th</sup> plane was created to verify the calibration results. The verification could also be done in a 3D space without loss of generality. The 4<sup>th</sup> plane was generated by rotating the first plane  $5^\circ$  about the  $x$  axis and  $10^\circ$  about the  $y$  axis translated 0.5m along the  $z$  axis.

In the second setup, the angles between the planes were deliberately increased to see if it would improve the condition number of the Identification Jacobian. The detailed operations are given in Table 1. For the same purpose, in the third setup, the angles between the planes were made very small to see if the results became worse. In the fourth setup, the three planes were made all parallel to each other to form a singular configuration. Simulations were done to see if the calibration algorithm diverged in such a case.

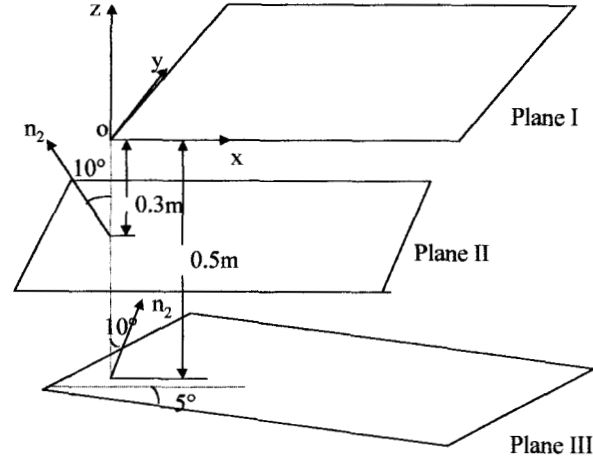


Figure 5 Setup 1 for the three planes

In the above figure,  $n_2$  and  $n_3$  are the normals of plane II and plane III respectively.

Table 1 Setup of the three planes

	Plane Setup	Set I	Set II	Set III	Set IV
Plane II	Rotation angles about $x$ axis	$10^\circ$	$40^\circ$	$1^\circ$	$0^\circ$
	Rotation angles about $y$ axis	$0^\circ$	$0^\circ$	$0^\circ$	$0^\circ$
	Distance between the origin and the plane (m)	0.5	0.5	0.1	0.1
Plane III	Rotation angles about $x$ axis	$-10^\circ$	$-50^\circ$	$-1^\circ$	$0^\circ$
	Rotation angles about $y$ axis	$5^\circ$	$30^\circ$	$2^\circ$	$0^\circ$
	Distance between the origin and the plane (m)	0.3	0.3	0.1	0.2
Plane IV	Rotation angles about $x$ axis	$5^\circ$	$5^\circ$	$5^\circ$	$5^\circ$
	Rotation angles about $y$ axis	$10^\circ$	$10^\circ$	$10^\circ$	$10^\circ$
	Distance between the origin and the plane (m)	0.5	0.5	0.5	0.5

The nominal parameters of the PUMA560 robot are listed in Table 2. These values were adopted from [ 7 ]. The simulated actual values of these parameters were obtained by randomly adding 0.01mm to the distance parameters and  $0.01^\circ$  to the angular

parameters. According to the definition of the coordinates systems, there were 24 parameters to be calibrated, including  $d_0, \alpha_0, \theta_1, a_1, \alpha_1, \theta_2, a_2, \alpha_2, \beta_2, \theta_3, d_3, a_3, \alpha_3, \theta_4, d_4, a_4, \alpha_4, \theta_5, d_5, a_5, \alpha_5, \theta_6, d_6, a_6$ . By applying the Singular Value Decomposition (SVD) on the Identification Jacobian, it was found that within these 24 parameters, only 23 were identifiable. This observation was agreeable with that of [ 7 ]. Therefore,  $\alpha_4$  was excluded.

Table 2 Establishing coordinate systems for the calibration of a PUMA560 robot

PUMA robot arm link and planar coordinate parameters					
$i$	$\theta_i$ (deg)	$d_i$ (mm)	$a_i$ (mm)	$\alpha_i$ (deg)	$\beta_i$ (deg)
0	0	740.0	0	90.0	0
1	0.0	0	0.0	-90.0	0
2	0.0	0	431.8	0.0	0.0
3	0.0	149.09	-20.32	90.0	0
4	0.0	433.07	0.0	-90.0	0
5	0.0	0.0	0.0	90.0	0
6	0.0	175.25	-12.0	0	0

In the simulations, different levels of uniformly distributed noise were inserted to the joint angular measurements to simulate different accuracy of the measurements. Three types of noise are listed in Table 3. Type I represents relatively accurate joint measurements while type III represents very rough measurements. Uniformly distributed random noise of 10  $\mu m$  was injected to the points from the planes to represent the flatness and roughness of the planes.

Table 3 Noise intensity of the joint angular measurements

	Type I	Type II	Type III
Noise intensity in joint angles( $\mu rad$ )	50	100	150
Noise intensity in plane roughness and smoothness ( $\mu m$ )	10	10	10

Forty points were chosen on each calibration plane. These points were randomly distributed in a  $0.8 \times 1 \text{m}^2$  area on each plane. Twenty points were generated on the 4<sup>th</sup> plane to verify the calibration results. A numerical inverse kinematic model was used to calculate the 6 joint angular measurements corresponding to each point on the planes. A nonlinear least squares algorithm was applied to estimate the error parameter vector  $d\rho_a$ . After  $d\rho_a$  was obtained, it was used to modify the parameter vector and in turn to compute the end-effector positions of the robot on the 4<sup>th</sup> plane. These positions were compared with the “actual” positions to determine the accuracy the calibration results.

### 5.3 Simulation Results

Figure 6 shows the simulation result when type I noise was added to the simulation, the three planes were placed as in setup I in Table 1. The nominal values of the parameters were illustrated in Table 2. In the graph, the  $x$  axis represents the number of measurements used in the calibration, and the  $y$  axis the norms of the difference between the calculated and the actual end-effector coordinates. In some of the simulations, the total number of measurements used in the calibration ranged from 110 to 120. This is to investigate the influence of the number of measurements used in the calibration on the system performance. Once the algorithm converges, the number of measurements used in the calibration has very little effect on the system performance, as shown in Figure 6. It also shows that the system achieved a best accuracy of 0.08mm when type I noise was added to the system.

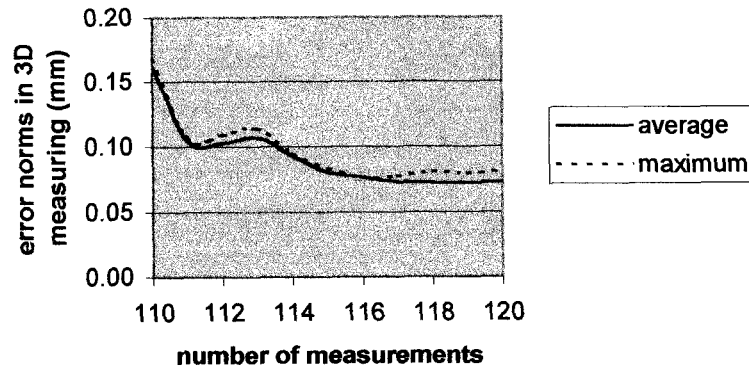


Figure 6 Simulation results when type I noise is added

Types II and III noise represent relatively more crude angular measurements. Figure 7 and Figure 8 show the simulation results respectively. When type II noise is added, the best system performance achieved is 0.18mm which is bigger than that of type I noise. This is understandable since type II noise is larger than type I noise. When type III noise is added, the system performance reaches 0.21mm. In all of the above cases, the condition number is between 200 and 500, which implies a well conditioned numerical system.

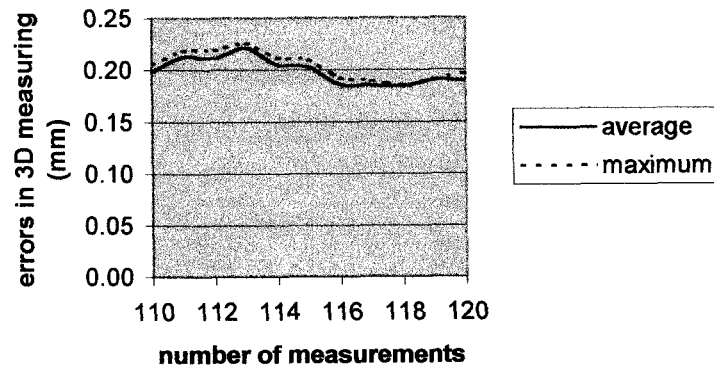


Figure 7 Simulation results when type II noise is added

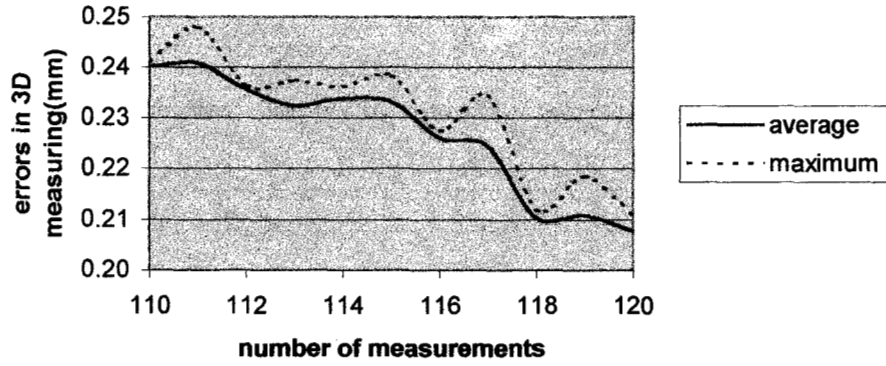


Figure 8 Simulation results when type II noise is added

Setups II, III and IV in Table 1 were used to investigate the robustness of the algorithm by varying the orientations of the planes. The results are summarized in Table 4.

Table 4 Simulation results of different system setups

System Setup	Setup I	Setup II	Setup III	Setup IV
Mean Error Norm ( <i>mm</i> )	0.08	0.07	0.20	diverge

The above simulations demonstrated that the calibration strategy using plane constraints is feasible. When the angles between the orientations of different planes are relatively larger, the simulation results tend to be slightly better. When the three planes are placed almost parallel to each other, the simulation results severely deteriorates. If the three planes are parallel to each other which conflicts with the necessary conditions for the constrained system to be observable, the simulation algorithm diverges.

## 6 Summary

In this paper, issues related to robot calibration with planar constraints are investigated. The observability of the robot calibration with single-plane and multiple-plane constraints are respectively explored. It is shown that a single-plane constraint is normally not sufficient to calibrate a robot. It is also shown that by using a three-plane constraint, the constrained system is equivalent to an unconstrained point-measurement system under certain conditions. The significance of this observation is that one can use this setup to successfully calibrate a robot. Simulations have been conducted to verify the theory presented in the paper.

### Appendix: Proof of Theorem 1

**Proof:** It is assumed that the plane parameters are known *a priori*. For the sake of convenience, the plane equations are cited again here:

$$\mathbf{n}_s^T \mathbf{r} + d_s = 0, \quad s = 1, 2, 3 \quad (13)$$

Similar to the single-plane case, we define the augmented machine parameter vector  $\rho_a = [\rho^T, \alpha^T, \mathbf{p}^T]^T$ , where  $\alpha$  and  $\mathbf{p}$  represent the orientation and position of the machine base system in the reference coordinate system.  $\rho$  is the parameter vector of the machine. The target position is a function of the augmented tracker parameter vector  $\rho_a$  and the joint vector  $\theta$ ; that is

$$\mathbf{n}_s^T \mathbf{r}(\rho_a, \theta) + d_s = 0, \quad s = 1, 2, 3 \quad (14)$$

Let  $\rho_a = \rho_a^0 + d\rho_a$  where  $\rho_a^0$  is the initial augmented parameters of the tracker. Perturbing both sides of (14), we get

$$-\mathbf{n}_s^T \mathbf{J}(\rho_a^0, \theta) d\rho_a = \mathbf{n}_s^T \mathbf{r}(\rho_a^0, \theta) + d_s \quad (15)$$

where  $\mathbf{J} \equiv \nabla \mathbf{r}$ .

Since the plane parameters are known, we choose the three plane normal  $\mathbf{n}_1, \mathbf{n}_2, \mathbf{n}_3$  to be independent. In such case, there exists a nonsingular matrix  $\mathbf{A}$  such that

$$\mathbf{A}\mathbf{n}_1 = \begin{bmatrix} 1 \\ 0 \\ 0 \end{bmatrix} = \mathbf{e}_1 \quad \mathbf{A}\mathbf{n}_2 = \begin{bmatrix} 0 \\ 1 \\ 0 \end{bmatrix} = \mathbf{e}_2 \quad \mathbf{A}\mathbf{n}_3 = \begin{bmatrix} 0 \\ 0 \\ 1 \end{bmatrix} = \mathbf{e}_3 \quad (16)$$

Therefore,

$$\mathbf{A}[\mathbf{n}_1 \quad \mathbf{n}_2 \quad \mathbf{n}_3] = \mathbf{I} \quad (17)$$

$$\mathbf{A} = [\mathbf{n}_1 \quad \mathbf{n}_2 \quad \mathbf{n}_3]^{-1} \quad (18)$$

Let us pick  $m$  points at random on each of the 3 planes. With a total of  $3m$  measurements, the Jacobian of the constrained system is

$$\begin{bmatrix} \mathbf{n}_1^T & 0 & 0 & \cdots & 0 & 0 & 0 \\ 0 & \mathbf{n}_2^T & 0 & \cdots & 0 & 0 & 0 \\ 0 & 0 & \mathbf{n}_3^T & \cdots & 0 & 0 & 0 \\ \vdots & \vdots & \vdots & \ddots & \vdots & \vdots & \vdots \\ 0 & 0 & 0 & \cdots & \mathbf{n}_1^T & 0 & 0 \\ 0 & 0 & 0 & \cdots & 0 & \mathbf{n}_2^T & 0 \\ 0 & 0 & 0 & \cdots & 0 & 0 & \mathbf{n}_3^T \end{bmatrix}_{3m \times 9m} \begin{bmatrix} \mathbf{J}_1 \\ \mathbf{J}_2 \\ \mathbf{J}_3 \\ \vdots \\ \mathbf{J}_{1m} \\ \mathbf{J}_{2m} \\ \mathbf{J}_{3m} \end{bmatrix}_{9m \times \rho_a}$$

$$= \begin{bmatrix} (A^{-1}e_1)^T & 0 & 0 & \cdots & 0 & 0 & 0 \\ 0 & (A^{-1}e_2)^T & 0 & \cdots & 0 & 0 & 0 \\ 0 & 0 & (A^{-1}e_3)^T & \cdots & 0 & 0 & 0 \\ \vdots & \vdots & \vdots & \ddots & \vdots & \vdots & \vdots \\ 0 & 0 & 0 & \cdots & (A^{-1}e_1)^T & 0 & 0 \\ 0 & 0 & 0 & \cdots & 0 & (A^{-1}e_2)^T & 0 \\ 0 & 0 & 0 & \cdots & 0 & 0 & (A^{-1}e_3)^T \end{bmatrix}_{3m \times 9m} \begin{bmatrix} J_1 \\ J_2 \\ J_3 \\ \vdots \\ J_{1m} \\ J_{2m} \\ J_{3m} \end{bmatrix}_{9m \times \rho_a}$$

$$= E_{3m \times 9m} F_{9m \times 9m} \begin{bmatrix} J_1 \\ J_2 \\ J_3 \\ \vdots \\ J_{1m} \\ J_{2m} \\ J_{3m} \end{bmatrix}_{9m \times \rho_a}$$

where

$$E_{3m \times 9m} \equiv \begin{bmatrix} e^{-T} & 0 & 0 & \cdots & 0 & 0 & 0 \\ 0 & e^{-T} & 0 & \cdots & 0 & 0 & 0 \\ 0 & 0 & e^{-T} & \cdots & 0 & 0 & 0 \\ \vdots & \vdots & \vdots & \ddots & \vdots & \vdots & \vdots \\ 0 & 0 & 0 & \cdots & e^{-T} & 0 & 0 \\ 0 & 0 & 0 & \cdots & 0 & e^{-T} & 0 \\ 0 & 0 & 0 & \cdots & 0 & 0 & e^{-T} \end{bmatrix}_{3m \times 9m}$$

and

$$F_{9m \times 9m} \equiv \begin{bmatrix} A^{-T} & 0 & 0 & \cdots & 0 & 0 & 0 \\ 0 & A^{-T} & 0 & \cdots & 0 & 0 & 0 \\ 0 & 0 & A^{-T} & \cdots & 0 & 0 & 0 \\ \vdots & \vdots & \vdots & \ddots & \vdots & \vdots & \vdots \\ 0 & 0 & 0 & \cdots & A^{-T} & 0 & 0 \\ 0 & 0 & 0 & \cdots & 0 & A^{-T} & 0 \\ 0 & 0 & 0 & \cdots & 0 & 0 & A^{-T} \end{bmatrix}_{9m \times 9m}$$

Note that  $F_{9m \times 9m}$  is nonsingular if  $A$  is non-singular. Since  $\mathbf{n}_1, \mathbf{n}_2, \mathbf{n}_3$  are independent,  $A$  is non-singular. Now  $F_{9m \times 9m}$  is nonsingular, it follows that

$$\text{rank}(E_{3m \times 9m} \begin{bmatrix} \mathbf{J}_1 \\ \mathbf{J}_2 \\ \mathbf{J}_3 \\ \vdots \\ \mathbf{J}_{1m} \\ \mathbf{J}_{2m} \\ \mathbf{J}_{3m} \end{bmatrix}_{9m \times \rho_a}) = \text{rank}(\begin{bmatrix} \mathbf{J}_{1x} \\ \mathbf{J}_{2y} \\ \mathbf{J}_{3z} \\ \vdots \\ \mathbf{J}_{(3m-2)x} \\ \mathbf{J}_{(3m-1)y} \\ \mathbf{J}_{3mz} \end{bmatrix}) \quad (19)$$

Since

$$E_{3m \times 9m} \begin{bmatrix} J_1 \\ J_2 \\ J_3 \\ \vdots \\ J_{(3m-2)} \\ J_{(3m-1)} \\ J_{3m} \end{bmatrix} = \begin{bmatrix} J_{1x} \\ J_{2y} \\ J_{3z} \\ \vdots \\ J_{(3m-2)x} \\ J_{(3m-1)y} \\ J_{3mz} \end{bmatrix}$$

It follows that the full set of error parameters can be made observable if matrix

$$\begin{bmatrix} J_{1x} \\ J_{2y} \\ J_{3z} \\ \vdots \\ J_{(3m-2)x} \\ J_{(3m-1)y} \\ J_{3mz} \end{bmatrix}$$

is non-singular.

Q.E.D.

#### Reference:

- [ 1 ] Mooring, B. W., Z. S. Roth, and M. Driels, *Fundamentals of manipulator calibration*, pp 23-48, John Wiley & sons, Inc.
- [2] Zhuang, H., L. Liu, and O. Masory, "Self-calibration of hexapod machine tools," *ASME J. Manufacturing Science and Technology*, Feb. 2000, pp. 140-148.
- [3] Zhuang, H., "Self-calibration of parallel mechanism with a case study on Stewart platforms," *IEEE Trans. Robotics & Automation*, Vol. 13, No. 3, June 1997, pp. 387-397.
- [ 4 ] Bennett, D. J. and J. Hollerbach, "Autonomous calibration of single-loop closed kinematic chains formed by manipulators with passive joints," *IEEE Trans. Robotics & Automation*, Vol. 7, No. 5, pp. 597-606.
- [ 5 ] Mooring, B. W., "Calibration of a laser projection system," *ASME*, DSC-Vol. 29, pp 33-41, 1991.
- [ 6 ] Zhuang, H., B. Li, Z. S. Roth, and X. Xie, "Self-calibration and mirror center offset

elimination of a multi-beam laser tracking system," *Robotics and Autonomous Systems*, Vol.9, pp. 255-269, 1992.

- [ 7 ] Ikits, M. and J. Hollerbach, "Kinematic calibration using a plane constraint," Proc. *IEEE Intl. Conf. Robotics & Automatiion*, pp. 3191-3196, April 20-25, 1997.
- [ 8 ] Khalil, W. and S. Besnard, "Self calibration of Stewart-Gough parallel robots without extra sensors," *IEEE Trans. Robotics & Automation*, Vol. 15, No. 6, pp. 1116-1121, 1999.
- [ 9 ] Zhuang, H. and Z. S. Roth, *Camera Aided Robot Calibration*, CRC Press, 1996.
- [10] Motaghedi, S. H., *Self-calibration of Laser Tracking Measurement System with Planar Constraints*, Ph.D. Dissertation, Florida Atlantic University, Boca Raton, FL, 1999.